ESC European Society of Cardiology

Cardiovascular Research (2023) **119**, 1441–1452
https://doi.org/10.1093/cvr/cvac121

Quantifying the impact of gut microbiota on inflammation and hypertensive organ damage

Ellen G. Avery [1,2,3,4†], Hendrik Bartolomaeus [1,2,3,5†], Ariana Rauch [1,2,3,5], Chia-Yu Chen [1,2,3,6], Gabriele N'Diaye[1,2,6], Ulrike Löber [1,2,3], Theda U. P. Bartolomaeus [1,2,3,6], Raphaela Fritsche-Guenther [2,7], André F. Rodrigues [2,3,4], Alex Yarritu[1,2,3,5], Cheng Zhong[8], Lingyan Fei[8], Dmitry Tsvetkov [1,3,6,9], Mihail Todiras [2,10], Joon-Keun Park[11], Lajos Markó [1,2,3,6], András Maifeld[1,2,3,6], Andreas Patzak[8], Michael Bader [2,3,6], Stefan Kempa [2,12], Jennifer A. Kirwan [2,7], Sofia K. Forslund [1,2,3,6], Dominik N. Müller [1,2,3,6]*, and Nicola Wilck [1,2,3,5]*

[1]Experimental and Clinical Research Center, A Cooperation of Charité-Universitätsmedizin Berlin and Max-Delbrück-Center for Molecular Medicine, Berlin, Germany; [2]Max-Delbrück-Center for Molecular Medicine in the Helmholtz Association, Berlin, Germany; [3]DZHK (German Centre for Cardiovascular Research), partner site Berlin, Germany; [4]Department of Biology, Chemistry, and Pharmacy, Freie Universität Berlin, Berlin, Germany; [5]Department of Nephrology and Internal Intensive Care Medicine, Charité-Universitätsmedizin Berlin, Corporate member of Freie Universität Berlin and Humboldt-Universität zu Berlin, Berlin, Germany; [6]Charité-Universitätsmedizin Berlin, Corporate member of Freie Universität Berlin and Humboldt-Universität zu Berlin, Berlin, Germany; [7]Metabolomics Platform, Berlin Institute of Health at Charité-Universitätsmedizin Berlin, Berlin, Germany; [8]Institute of Translational Physiology, Charité-Universitätsmedizin Berlin, Corporate Member of Freie Universität Berlin and Humboldt-Universität zu Berlin, Charitéplatz 1, 10117 Berlin, Germany; [9]Department of Geriatrics, University of Greifswald, University District Hospital Wolgast, Greifswald, Germany; [10]Nicolae Testemianu State University of Medicine and Pharmacy, Chisinau, Moldova; [11]Hannover Medical School, Hannover, Germany; and [12]Integrative Proteomics and Metabolomics Platform, Berlin Institute for Medical Systems Biology BIMSB, Berlin, Germany

Received 23 September 2021; revised 4 July 2022; editorial decision 8 July 2022; online publish-ahead-of-print 29 July 2022

Time of primary review: 44 days
This article was guest edited by Thomas F. Lüscher.

Aims Hypertension (HTN) can lead to heart and kidney damage. The gut microbiota has been linked to HTN, although it is difficult to estimate its significance due to the variety of other features known to influence HTN. In the present study, we used germ-free (GF) and colonized (COL) littermate mice to quantify the impact of microbial colonization on organ damage in HTN.

Methods and results 4-week-old male GF C57BL/6J littermates were randomized to remain GF or receive microbial colonization. HTN was induced by subcutaneous infusion with angiotensin (Ang) II (1.44 mg/kg/day) and 1% NaCl in the drinking water; sham-treated mice served as control. Renal damage was exacerbated in GF mice, whereas cardiac damage was more comparable between COL and GF, suggesting that the kidney is more sensitive to microbial influence. Multivariate analysis revealed a larger effect of HTN in GF mice. Serum metabolomics demonstrated that the colonization status influences circulating metabolites relevant to HTN. Importantly, GF mice were deficient in anti-inflammatory faecal short-chain fatty acids (SCFA). Flow cytometry showed that the microbiome has an impact on the induction of anti-hypertensive myeloid-derived suppressor cells and pro-inflammatory Th17 cells in HTN. *In vitro* inducibility of Th17 cells was significantly higher for cells isolated from GF than conventionally raised mice.

Conclusion The microbial colonization status of mice had potent effects on their phenotypic response to a hypertensive stimulus, and the kidney is a highly microbiota-susceptible target organ in HTN. The magnitude of the pathogenic response in GF mice underscores the role of the microbiome in mediating inflammation in HTN.

Keywords Hypertension • Microbiome • Inflammation • Kidney • Heart

* Corresponding authors. Tel: +49 30 450540459, E-mail: nicola.wilck@charite.de (N.W.); Tel: +49 30 450540286, E-mail: dominik.mueller@mdc-berlin.de (D.N.M.)
† These authors contributed equally.

1. Introduction

Hypertension (HTN) is the leading risk factor for non-communicable diseases worldwide,[1] and is known as a multifactorial disease, where complex mechanisms often co-occur to lead to a persistent increase in blood pressure (BP). Several studies have indicated that alterations in the composition and function of the intestinal microbiota may contribute to the burden of hypertensive disease.[2–6] However, it is difficult to estimate the contribution of the microbiota, especially in human studies, where the added complexities of other contributing factors easily obstruct our understanding. The aim of our study is to understand the relative contribution that the microbiota has to the burden of hypertensive disease.

Mounting evidence suggests that inflammation is not only characteristic of hypertensive cardiovascular disease (CVD) but is causally linked to disease progression and severity.[3] Components of both the innate and adaptive immune system have been implicated.[3] T-helper 17 (Th17) cells and Type 1 helper T-cells (Th1) have been shown to be integrally interlinked with hypertensive disease, and have been demonstrated to exacerbate cardiac and renal damage.[5,7,8] Moreover, myeloid-derived suppressor cells (MDSCs) derived from hypertensive mice were shown to have immunosuppressive properties, and upon adoptive transfer were able to mitigate BP increase in response to angiotensin II (Ang II) infusion.[9] MDSC, Th17, and Th1 cells have each been shown in different settings to be influenced by the microbiota.[5,9–11]

We and others could recently demonstrate the role of several anti-inflammatory microbial metabolites in HTN. Short-chain fatty acids (SCFA) such as acetate, propionate, and butyrate, are produced by gut microbiota through the fermentation of indigestible dietary fibre.[12] Acetate has been shown to ameliorate hypertensive damage to the kidney and heart in mice.[13] Our recent work elucidated the protective role of propionate in Ang II-induced inflammation and cardiovascular damage.[14] Furthermore, low butyrate levels have been associated with worsened CVD in several models.[15] In addition to SCFA, we have recently shown that a bacterially produced indole metabolite derived from tryptophan suppresses Th17-driven inflammation in salt-sensitive HTN.[5] In contrast, metabolites of microbial origin can also exacerbate disease in some contexts. For example, pro-inflammatory metabolites like trimethylamine N-oxide (TMAO) and indoxyl sulfate (IS) have been shown to aggravate CVD.[16,17]

To address our central aim, we utilized germ-free (GF) mice. C57BL/6J GF littermates were randomized at 4 weeks of age to either receive a microbiota transfer from our in-house C57BL/6J colony, or to remain GF for the duration of the experiment. Here, we have uncovered several differences between GF and colonized (COL) mice in response to Ang II and 1% NaCl in the drinking water, which underscores the importance of the microbiota in the pathogenesis of HTN-induced organ damage. Of note, we show an exacerbation of damage in GF mice compared with COL mice, which is more distinct in the kidney than in the heart.

2. Materials and Methods

Detailed description of all analytical methods and data analysis used are available in the Supplementary material online.

2.1 Animal ethics

All experiments performed complied with the German/European law for animal protection and were approved by the local ethics committee (G0280/13, G0028/21).

2.2 Animal protocol

Wild-type C57BL/6J mice were bred under axenic conditions in an isolator (Metall + Plastic, Radolfzell-Stahringen, Germany). Mice were maintained on a 12:12 h day: night cycle with constant access to food and water. Until Week 4, mice in both experimental groups grew under GF conditions. At 4 weeks of age, male mice were randomized to either remain GF in the isolator or receive passive bacterial colonization (COL). For colonization, mice were introduced in the regular SPF animal facility and placed in cages from healthy wild-type male C57BL/6J mice. Until 12 weeks of age mice received sterilized tap water as drinking water. At 12 weeks of age, COL and GF mice received Angiotensin II (Ang II, 1.44 mg/kg/day) by subcutaneous infusion via an osmotic minipump (Alzet) and 1% NaCl (Carl Roth) in the drinking water or sham treatment. Sham-treated animals received the same operation procedure without minipump implantation. Minipumps were implanted under sterile conditions, GF mice were kept sterile throughout the experiment. Sterile drinking water was delivered via the Hydropac system (Plexx B.V., Elst, the Netherlands). Throughout the experiment mice were fed autoclaved standard breeding chow (V1124, Ssniff, Soest, Germany). After 2 weeks of Ang II + 1% NaCl or sham treatment mice were euthanized by isoflurane anaesthesia and blood, spot urine (where possible), faeces, and organs were collected. The Ang II infusion model was performed in 40 mice (GF $n = 5$, COL $n = 5$, GF + HTN $n = 16$, COL + HTN $n = 14$). Over the course of the experiments, five animals were taken out of the experiment (GF + HTN $n = 3$, COL + HTN $n = 2$), due to pre-specified ethical termination criteria in order to counteract severe distress in this experiment. These five mice were not included in the analysis. Additionally, invasive BP measurements were performed in 10 animals (GF $n = 5$, COL $n = 5$), these animals were not included in any other analysis. As a control group for *in vitro* experiments, cells, and tissues from age-matched conventionally raised SPF C57BL/6J mice (referred to as CONV) were used.

Mice were euthanized by isoflurane anaesthesia (5% isoflurane–air mixture). Furthermore, echocardiography, BP, and Ang II pressor response measurements were performed in isoflurane inhalation anaesthesia (2–2.5% isoflurane–air mixture). Details are given in Supplementary material online.

3. Results

3.1 Absence of microbiota exacerbates cardiorenal damage

To exclude confounding effects relating to the genetic background of mice used in our study, GF littermates were randomized at 4 weeks of age for colonization with SPF microbiota (COL) or further kept under GF conditions. At 12 weeks of age, we induced HTN by subcutaneous Ang II infusion and 1% NaCl-supplemented drinking water. After 14 days, we analysed hypertensive target organ damage (*Figure 1A*). Of note, we did not include surgical uninephrectomy to avoid bacterial contamination. The standard model in our lab includes uninephrectomy to induce a more severe form of renal damage,[8,18] thus we expected a lower degree of renal damage when compared with the published literature.[19] To validate the integrity of our experiment, we first checked the colonization status of the mice. Gross morphological changes were assessed, and the characteristics typical of the gastrointestinal (GI) tract in GF mice (e.g. megacecum) did not persist in the mice which had been colonized (COL) (see Supplementary material online, *Figure S1A*). To confirm the microbial status of the respective group, we examined faecal pellets

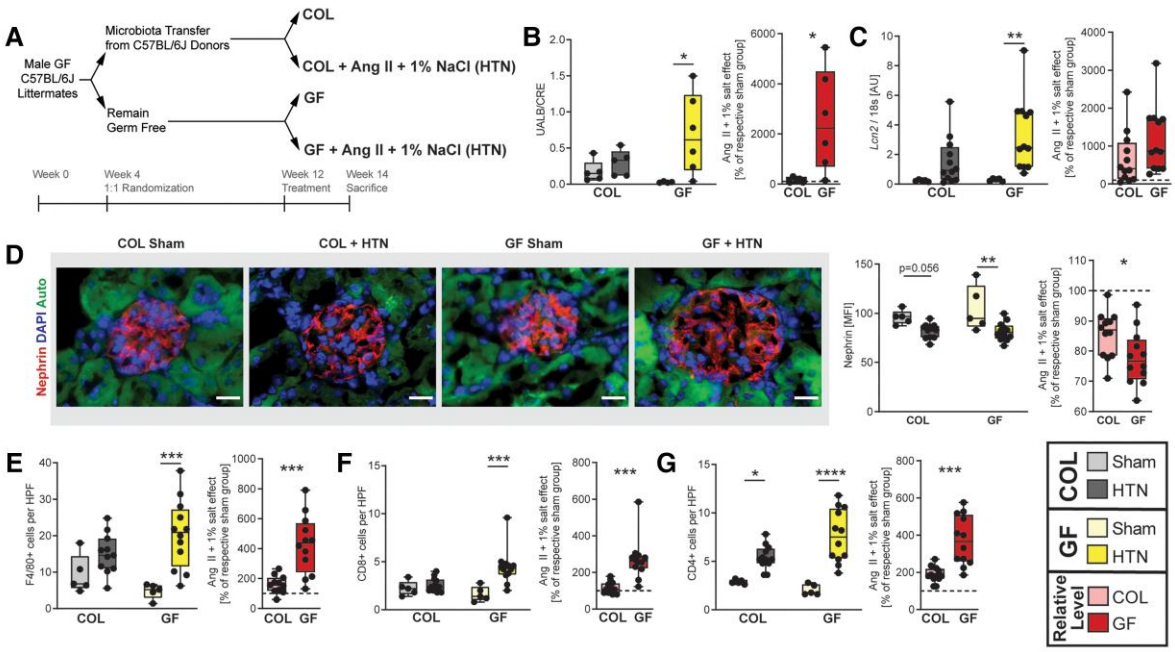

Figure 1 Renal damage is exacerbated under GF conditions. (*A*) Description of experimental protocol (unless otherwise stated, GF Sham $n = 5$, GF + HTN $n = 12$, COL Sham $n = 5$, COL + HTN $n = 12$ for further analyses). (*B*) Urinary albumin-to-creatinine ratio from spot urine collected upon sacrifice from a subset of mice (COL $n = 5$, COL + HTN $n = 5$, GF $n = 4$, GF + HTN $n = 6$). (*C*) *Lcn2* gene expression was measured from kidney tissue by qPCR. (*D*) Histological kidney sections were stained for nephrin. Representative glomeruli are shown (left). Nephrin immunofluorescence was quantified as mean fluorescence intensity (MFI) in the glomerular space averaged per mouse. The scale bar represents 20 µm. (*E*) Macrophages (F4/80+), (*F*) CD8+, and (*G*) CD4+ T-cells from kidney sections were counted from five representative high-power fields within the cortex. For (*B–G*), the left graph was tested using a two-way ANOVA and *post hoc* Sidak multiple comparison's test and depicts the raw values for each variable. For (*B–F*), HTN was identified as the source of variation using two-way ANOVA, and *post hoc* multiple comparison between sham and HTN within each group revealed that the GF comparison was the source of variation. In (*G*), HTN was identified as the source of variation using two-way ANOVA, and *post hoc* multiple comparison between sham and HTN within each group revealed that both the GF and COL comparison were significant. For *B* through *G*, the right plot depicts the relative change induced by Ang II + 1% NaCl in comparison with the respective sham group, tested using an unpaired two-tailed *t*-test. No change (100%) depicted as dotted line. For all plots, *P*-values are as follows; $*P \leq 0.05$, $**P \leq 0.01$, $***P \leq 0.001$, $****P \leq 0.0001$.

produced on the final day of experimentation. First, pellets were incubated in a thioglycolate medium for 96 h, and GF mice were found to show no bacterial growth (see Supplementary material online, *Figure S1B*). Second, 16S rDNA copies per gram stool measured by qPCR were found to be similar in COL (Sham and HTN) and conventional SPF mice (CONV), whereas GF mice did not have more 16S rDNA copies than blank samples (see Supplementary material online, *Figure S1C*). Finally, unimputed serum metabolomics confirmed the presence of bacterially-derived metabolites in COL mice only (see Supplementary material online, *Figure S1D*). Shotgun metagenomics revealed that the grafted bacteria in COL mice showed the largest overlap with mouse gut metagenomes published in the global microbial gene catalogue (GMGC) (see Supplementary material online, *Figure S2*). We therefore concluded that the GF and COL groups were maintained as intended to confidently proceed with further analyses. Of note, it has been previously reported for the Ang II infusion model that HTN induction leads to changes in the microbiome composition.[20] Likewise, we found Ang II infusion influenced the abundance of various taxa in COL mice (see Supplementary material online, *Figure S1E*) as shown by shotgun sequencing. Indeed, both the caecal and faecal compartments displayed differences between the COL sham and HTN groups on phylum and genus levels (see Supplementary material online, *Figure S1F* and *G*, and *File S1–4*).

One of the hallmarks of hypertensive target organ damage is renal damage, which is characterized by abnormally high excretion of albumin with the urine (albuminuria), fibrosis, and inflammation. In line with the literature,[19] our HTN induction without uninephrectomy lead to a moderate increase in albuminuria in COL mice (*Figure 1B*). GF mice developed a greater degree of albuminuria upon HTN induction, which is abundantly clear when comparing the relative increase of GF and COL mice compared with their respective sham groups (*Figure 1B*). HTN also lead to a significant increase in renal damage marker lipocalin-2 in GF mice (Lcn2), which was not evident in COL mice (*Figure 1C*). Next, we analysed nephrin, a protein in the podocytes' slit membrane, by immunofluorescence. We observed a significant decrease of nephrin immunofluorescence in GF mice, where COL mice exhibited a similar but insignificant trend (*Figure 1D*). HTN led to a significant increase of macrophages (F4/80+ cells, *Figure 1E*) and cytotoxic T-cells (CD8+ cells, *Figure 1F*) in the kidney of GF mice, not reaching significance in COL mice. Likewise, we found that mRNA expression of CC-chemokine ligand 2 (Ccl2, see Supplementary material online, *Figure S3A*) and infiltrating T-cells (CD3+, see Supplementary material online, *Figure S3B*) were selectively increased in the GF group upon HTN. While T-helper cells (CD4+ cells) were shown to increase in both GF and COL mice, GF mice displayed a stronger increase

(*Figure 1G*). The number of leukocytes (CD45+ cells) within the kidney confirms the stronger effect of HTN on renal inflammation in GF (see Supplementary material online, *Figure S3C*). For all immune populations in the kidney, the change in HTN relative to sham was consistently exacerbated in GF compared with COL (*Figure 1E–G*, and see Supplementary material online, *Figure S3B and C*). Finally, we investigated kidney fibrosis. Expression of *Col3a1* was significantly increased only in GF + HTN mice (see Supplementary material online, *Figure S3D*). Perivascular fibrosis analysed by Masson's trichrome staining was accentuated in GF mice but not statistically different between the groups using two-way analysis of variance (ANOVA); although when comparing the relative increase from sham to HTN, there was a significant difference between GF and COL (see Supplementary material online, *Figure S3E*). Similar to what was previously shown,[21] GF mice tended to have lower baseline values for several damage markers when comparing sham-treated GF and COL mice. Overall, renal pathology upon HTN induction was greater in GF mice when compared with their COL littermates.

Next, we examined the cardiac phenotype. HTN induction led to greater hypertrophy in GF compared with COL mice, as measured by heart weight-to-tibia length ratio (*Figure 2A*). Left ventricular weight taken from echocardiography relative to the tibia length (*Figure 2B*) as well as cardiac *Nppb* expression (*Figure 2C*) confirmed this finding. Neither the GF + HTN nor COL + HTN mice had a reduced ejection fraction (*Figure 2D*), indicating none of these mice were experiencing systolic heart failure. Using two-way ANOVA, both perivascular (*Figure 2E*) and interstitial (*Figure 2F*) fibrosis were significantly increased in GF + HTN and not in COL + HTN mice compared with their respective sham group. Interestingly, when assessing the relative increase in HTN compared with sham for markers of cardiac fibrosis, there was no difference in GF compared with COL mice (*Figure 2E and F*). Next, we examined cardiac inflammation. Despite an increase in *Ccl2* expression in GF and not COL (see Supplementary material online, *Figure S4A*), macrophages (F4/80+) were increased in both GF and COL hearts upon HTN; and GF + HTN showed significantly less macrophages than COL + HTN mice (*Figure 2G*). The change in overall leukocytes (CD45+) within the heart mimics the changes seen for macrophages (see Supplementary material online, *Figure S4B*). Furthermore, no significance was reached when comparing CD4+ T-helper cell infiltration (*Figure 2H*), whereas CD8+ cytotoxic T-cells in the hearts increased in both GF + HTN and COL + HTN mice compared with sham (*Figure 2I*). We also observed an increase in the cardiac expression of pro-inflammatory cytokine *Tnfa* selectively in the GF + HTN group compared with sham (see Supplementary material online, *Figure S4C*). Altogether, cardiac hypertrophy and inflammation following HTN were affected to a greater extent in GF, but when assessing the relative change for GF and COL mice in HTN compared with sham we saw many similarities in the development of the cardiac fibrosis. Whereas in the kidney, there was a clear difference in the development of HTN damage between GF and COL mice, these distinctions were less evident in the heart.

3.2 Hypertensive kidney damage is more sensitive to microbial status than cardiac damage

The aforementioned findings indicate that GF mice respond more sensitively to HTN. Within the context of our initial statistical approach (two-way ANOVA) we often saw a loss of significance for the HTN effect in COL mice under equal statistical power; and the differences between GF and COL response where much clearer when assessing the relative increase for a given marker in HTN (unpaired *t*-test). To expand on this idea to increase our understanding of the differences between GF and COL, we assessed the size of the HTN-induced effect by calculating an effect size (Cliff's delta) and fold change for each marker. Using a comprehensive univariate testing strategy, we assessed the significance in the different tissue spaces using a robust false discovery rate (FDR) correction within GF and COL groups to root out any spurious findings. From the majority of kidney parameters assessed, across the subcategorizations of damage, fibrosis, and inflammatory markers, a very consistent pattern emerged in that the GF mice experienced worsened kidney outcomes compared with COL mice (*Figure 3A*, see Supplementary material online, *Table S1*). In contrast to the renal damage, both GF and COL mice experienced a more similar cardiac damage pattern, particularly regarding markers of cardiac fibrosis (*Figure 3B*, and see Supplementary material online, *Table S2*). Albeit several cardiac parameters reached significance in GF and COL mice, the fold changes observed in GF mice were often larger (e.g. *Nppb*, perivascular fibrosis, *Ccn2*, *Lcn2*, F4/80, CD8; see Supplementary material online, *Table S2*). GF + HTN mice develop a significant increase in lung weight-to-tibia length ratio (*Figure 3B*), indicating the development of lung congestion[22] due to aggravated cardiac dysfunction. Taken together, there was more overlap in the cardiac response to HTN in GF and COL groups than was seen for the kidney parameters.

To further quantify the HTN effect across the renal (*Figure 3C*) and cardiac (*Figure 3D*) tissue space, we performed a multivariate principal coordinate analysis (PCoA) summarizing the overall (dis)similarities amongst the groups. To assess pairwise comparisons of interest, the overall dataset was divided and tested using PERMANOVA (*Figure 3C*). The pairwise comparisons of the kidney phenotypic data show a significant distance in the COL group from sham to HTN (P-value = 0.012, F-value = 4.8). However, the effect of HTN, as measured by the F-value, was greater in the GF mice (P-value = 0.001, F-value = 8.2). In line with our initial univariate targeted analysis (*Figure 1*), this indicates that the overall phenotypic change in the kidney in response to HTN was larger in GF mice than in COL mice. Furthermore, the pairwise PERMANOVA between GF + HTN and COL + HTN groups (P-value = 0.044, F-value = 3.2) indicates that HTN induction resulted in a different outcome on a multivariate level. Despite some slight differences within some univariate kidney data in the sham groups (e.g. albuminuria, F4/80 + cells), pairwise comparison of GF and COL sham samples was insignificant (P-value = 0.262, F-value = 1.4).

For the multivariate analysis of our cardiac data, pairwise comparisons were also used to assess the trajectory of each group (*Figure 3D*). Consistent with our conclusions from the univariate assessment of the overall cardiac phenotype (*Figure 3B*), we saw that the comparison between GF + HTN and COL + HTN group showed significant overlap in the PCoA plot, and the pairwise comparison between these samples was not significant (P-value = 0.391, F-value = 1.1). Conversely, the difference between sham GF and COL samples was significant, suggesting that perhaps the basal cardiac phenotype is sensitive to the host's microbiome status (P-value = 0.01, F-value = 5.6). As expected, the comparison of HTN with sham samples within the GF (P-value = 0.01, F-value = 4.8) and COL (P-value = 0.046, F-value = 3.2) samples were both significant. The cardiac data again indicate larger phenotypic shifts in GF mice most likely driven by significantly different sham groups.

Taken together, our univariate and multivariate approaches indicate a larger effect of HTN in GF mice. In the case of the kidney, this increased effect is indeed driven by a stronger adverse response of GF mice to

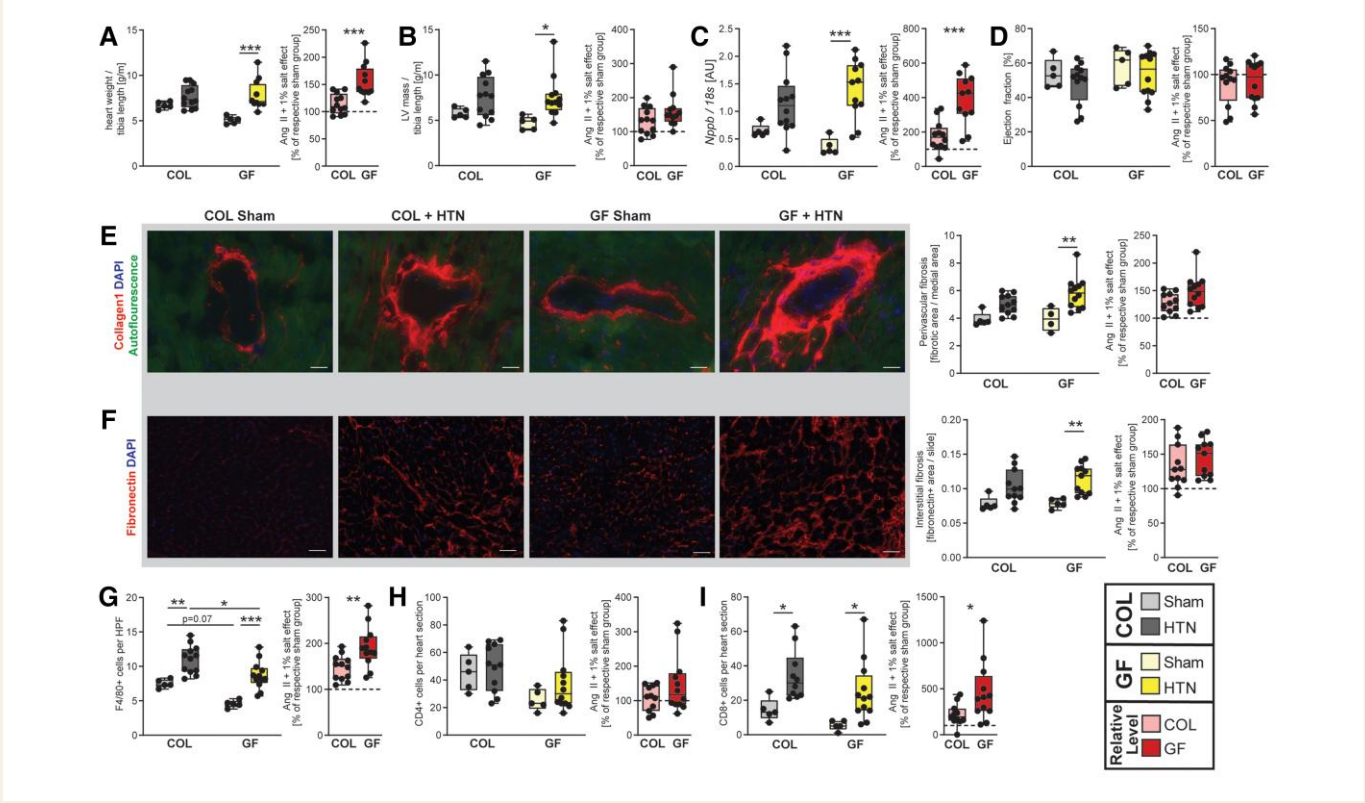

Figure 2 Cardiac inflammation and hypertrophy are aggravated in GF mice. Unless otherwise stated, GF Sham $n = 5$, GF + HTN $n = 12$, COL Sham $n = 5$, COL + HTN $n = 12$. (*A*) Heart weight-to-tibia length (g/m) from mice taken at sacrifice. (*B*) Left ventricular (LV) mass was estimated using echocardiography and normalized to tibia length (g/m). (*C*) Cardiac ventricular natriuretic peptide gene expression (*Nppb*) measured by qPCR. COL + HTN $n = 11$, otherwise as stated above. (*D*) Echocardiography prior to sacrifice revealed no change in the ejection fraction upon HTN induction in GF or COL mice. (*E*) Perivascular fibrosis from cardiac vessels, evaluated by measuring the fibrotic area relative to the medial area of vessels from Collagen 1-stained histology slides. GF Sham $n = 4$, otherwise as stated above. (*F*) Cardiac interstitial fibrosis was evaluated as fibronectin positive area proportionate to total area from five representative 40× magnification pictures from histological slides. In scale bar represents 40 µm. (*G*) Macrophages (F4/80+) were counted from five representative high-power fields, and (H) CD4+, and (*I*) CD8+ T-cells were counted from whole heart sections. Two-way ANOVA and *post hoc* Sidak multiple comparison's test for (*A–I*) was used to test significance in the left plot. In (*A–C*) and (*E and F*), HTN was identified as the source of variation using two-way ANOVA, and *post hoc* multiple comparison between sham and HTN within each group revealed that the GF comparison was the source of variation. In (*G*) HTN and the microbiome were both identified as sources of variation using two-way ANOVA, and significant *post hoc* comparisons are shown. In (*I*), HTN was identified as the source of variation using two-way ANOVA, and *post hoc* multiple comparison between sham and HTN within each group revealed that both the GF and COL comparison were significant. To the right in (*A–I*), the relative change induced by Ang II + 1% NaCl in comparison with the respective sham group was tested using an unpaired two-tailed *t*-test. No change (100%) depicted as dotted line. For all plots, *P*-values are as follows; $*P \leq 0.05$, $**P \leq 0.01$, $***P \leq 0.001$.

HTN, whereas in the case of the heart, this effect is driven by phenotypic differences in the healthy groups (sham-treated mice).

3.3 Vascular response to Angiotensin II is similar in GF and COL mice

There is some evidence from the literature that vascular reactivity may be dependent on microbial colonization.[23,24] We opted not to implant telemetry devices for the measurement of BP in our primary experimental animals, as microscopic vascular surgery was not possible under sterile conditions. Although we decided to forgo this gold-standard for BP measurement, we still questioned whether the axenic status of our GF mice would impact the basal mean arterial pressure (MAP), or BP reactivity to Ang II. We therefore colonized additional mice using the same colonization procedure as previously outlined, and we performed *in vivo* BP measurements using an implanted arterial catheter in freely moving mice. Interestingly, we found that GF mice had a significantly higher MAP (*Figure 4A*) than their colonized counterparts, although the mean of each group (GF mean value = 118.4 mmHg, COL mean value = 107.8 mmHg) was still in a range considered normal for untreated C57BL/6J mice.[25] Acute intravenous infusion of Ang II induced an increase in BP (*Figure 4B*) which was nearly identical for GF and COL mice, suggesting that Ang II-dependent reactivity of the vasculature is similar in these mice. Similarly, we investigated *ex vivo* vascular contractility of mesenteric arteries isolated from conventionally colonized mice (CONV) or GF mice (GF). CONV mice were used for this *in vitro* experiment due to ease of availability because colonization of GF mice is a lengthy procedure. GF mice showed similar contractile response compared with CONV mice in response to Ang II (see Supplementary material online, *Figure S5A*). Additionally, mesenteric arterial rings from GF mice showed similar contraction force in response to KCl to CONV mice (see Supplementary material online, *Figure S5B*). Similarly,

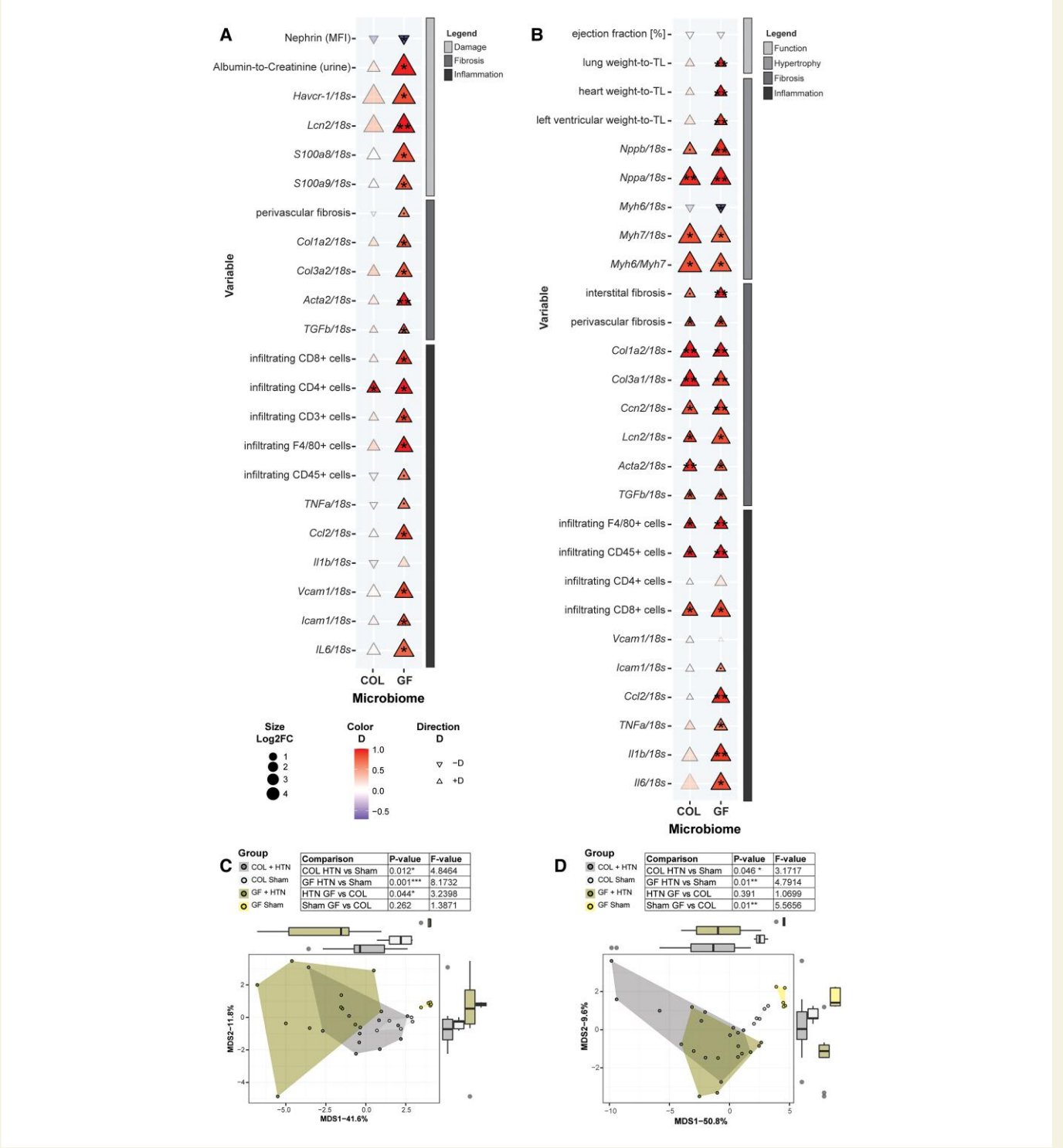

Figure 3 Unbiased assessment of kidney and heart damage in HTN-treated GF vs. COL mice. Unless otherwise stated, GF Sham $n = 5$, GF + HTN $n = 12$, COL Sham $n = 5$, COL + HTN $n = 12$. For cardiac RNA expression COL + HTN $n = 11$, otherwise as stated before. (*A*) Effect sizes [Cliff's delta (*D*)] and fold changes are shown to assess the effect of HTN treatment relative to the respective sham group in GF and COL on the kidney phenotype. Colour and triangle direction indicates effect size. Size indicates log2-transformed fold change (Log2FC) of HTN compared with the respective sham group. Significance was calculated using the Mann–Whitney *U*-test and was FDR-corrected with the Benjamini–Hochberg procedure to account for multiple testing. Markers for significant *Q*-values are superimposed, and transparency indicates non-significant effects. °$q < 0.1$, *$q < 0.05$, **$q < 0.01$. Variables are organized by subcategory (damage, fibrosis, inflammation). (*B*) Same univariate analysis as in (*A*) was performed on cardiac phenotypic data. Variables are organized by subcategory (function, hypertrophy, fibrosis, inflammation). (*C*) PCoA was performed based on Euclidean distance scaling of kidney phenotypic data to demonstrate the dissimilarities between study groups in a quantitative phenotypic state space (GF + HTN = 11, otherwise as stated). Pairwise comparisons between groups were preformed using PERMANOVA and reported in the inset table. (*D*) PCoA as in (*C*) was performed on the cardiac phenotypic data.

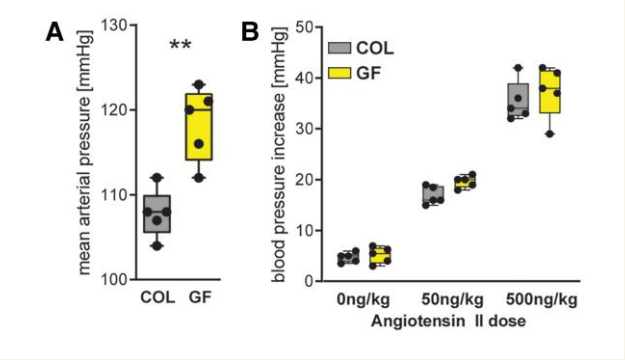

Figure 4 BP and Angiotensin II reactivity in GF and COL mice. $N = 5$ animals per group. (*A*) GF and COL mice were implanted an arterial catheter for BP measurement. MAP was measured in resting and awake animals, and the difference was tested using an unpaired two-tailed *t*-test (**$P \leq 0.01$). (*B*) The increase in BP after acute intravenous infusion of Angiotensin II as a bolus was measured. No statistical difference between GF and COL mice was found using a two-way repeated measurement ANOVA ($P = 0.14$), whereas Ang II dose had a significant influence ($P \leq 0.0001$, not shown).

endothelial-dependent (see Supplementary material online, *Figure S5C*) and –independent (see Supplementary material online, *Figure S5D*) relaxation was not influenced by colonization status.

3.4 Microbiota and microbial metabolites shape serum metabolome changes in HTN

Although the vascular reactivity of GF mice was similar to those housing microbes, we were interested to understand the different phenotypic and inflammatory response to HTN. We therefore decided to investigate the microbiome itself and associated metabolite production, as our group and others have previously shown that some metabolites of microbial origin can be anti-inflammatory in HTN.[5,13,14]

Consistent with the literature,[20] the metabolome of GF and COL animals was affected by HTN induction. We found a multitude of differences when analyzing the serum metabolome (MxP Quant 500, Biocrates) from GF and COL mice in HTN compared with the respective sham, which we grouped together by class to show the composite shift of over 300 individually measured metabolites (*Figure 5A*, and see Supplementary material online, *Table S3*). Of the 15 classes of metabolites where HTN induction had an effect, four of those classes (phosphatidylcholines, hexosylceramides, alkaloids, fatty acids) showed similar trajectories, suggesting these classes changed in a microbiome-independent manner upon HTN (*Figure 5A*, individual metabolites shown in see Supplementary material online, *Figure S6A–D*). For individual metabolites, we compared the impact of HTN induction on metabolite trajectories. When comparing sham with HTN, there was little overlap between the metabolites that decreased (*Figure 5B*) or increased (*Figure 5C*) within GF or COL. Overall, in GF mice more metabolites were regulated by HTN than in COL mice (see Supplementary material online, *Table S11*) (*Figure 5D*). Of note, a subset of metabolites which were upregulated in GF mice were downregulated in COL mice in response to HTN and vice versa (*Figure 5D*, shown in black). Taken together, the alterations of the metabolome in response to HTN show little overlap in GF and COL mice (*Figure 5D*, referred to as 'both'). Unsurprisingly, the serum metabolome was significantly impacted by the microbiome, and we saw a wide range of correlations between individual metabolites and microbial species, as well as functional modules derived from shotgun sequencing data (see Supplementary material online, *Figure S7*). Although the serum metabolite measurements used here were very comprehensive, they did not cover SCFA metabolites, which we and others have shown to have high importance in the progression of HTN. It has been demonstrated elsewhere that GF mice are devoid of some important SCFA.[26] We confirmed this for our mouse colonies (GF and CONV, which were the source populations for our experiments) by performing mass spectrometry measurements of faecal acetate, propionate, and butyrate (*Figure 5E*). We expect that the lack of the potent anti-hypertensive metabolites propionate and butyrate influences the phenotype seen in GF mice.

3.5 Inflammation contributes to the differing phenotypic response to HTN in GF and COL mice

It has been shown that the immune system and the gut microbiome are strongly interconnected, and several studies have shown the importance of immune cells in HTN.[2,3] We and others have also shown that metabolites of microbial origin can influence inflammation in HTN.[5,13,14] We examined the splenic immune cell composition a surrogate for systemic inflammation in GF and COL mice by flow cytometry (gating strategies are shown in see Supplementary material online, *Figure S8*). Of the 23 immune cell subsets we investigated, 12 were differentially influenced by HTN when compared with the respective sham group (*Figure 6A*, and see Supplementary material online, *Table S4*). We then examined all immune parameters multivariately to assess how changes in immune cells would be reflected in the distance between each group using PCoA (*Figure 6B*). It is known that the immune system of GF mice differs from their colonized counterparts.[27] Our data confirms this observation as the pairwise comparison of sham-treated GF and COL mice (*P*-value = 0.011, *F*-value = 6.6) was significant. Interestingly, this difference between COL and GF was still evident after HTN induction (*P*-value = 0.026, *F*-value = 2.8). Pairwise comparisons of individual groups using PERMANOVA indicated that the HTN to sham comparison was significant in the GF group (*P*-value = 0.006, *F*-value = 4.8), but not within the COL group (*P*-value = 0.177, *F*-value = 1.6) (*Figure 6B*). It can be concluded that overall, the inflammatory status of GF mice was disturbed to a greater degree by HTN induction.

Previous studies have shown that splenic MDSC increase in HTN and have anti-hypertensive properties.[9] In line with the literature, there was an increase in monocytic MDSC (mMDSC) upon HTN induction, and this increase was only significant in COL + HTN mice (*Figure 6C*). Furthermore, for both mMDSC and granulocytic MDSC (gMDSC) (*Figure 6D*) subtypes, COL + HTN mice showed a significantly higher frequency of these anti-hypertensive immune cells than GF + HTN mice. The relative increase in HTN compared with sham for mMDSC was lesser in GF mice but greater for gMDSC than in COL (*Figure 6C and D*). The dynamics of whether the relative increase, or absolute number of MDSCs is relevant in HTN is currently unknown. Additionally, we saw an increase in Th17 cells in both GF and COL mice, though this effect only reached significance in GF mice (*Figure 6E*). This increase was driven by pathological Th1-like Th17 cells, defined by their co-expression of RORgt and Tbet (*Figure 6F*).[28] Recent evidence suggest that pre-existing conditions can influence naive T-cell responses towards effector differentiation.[29–31] We hypothesized that the absence of microbes and their metabolites in GF mice would render naive T-cells more vulnerable to

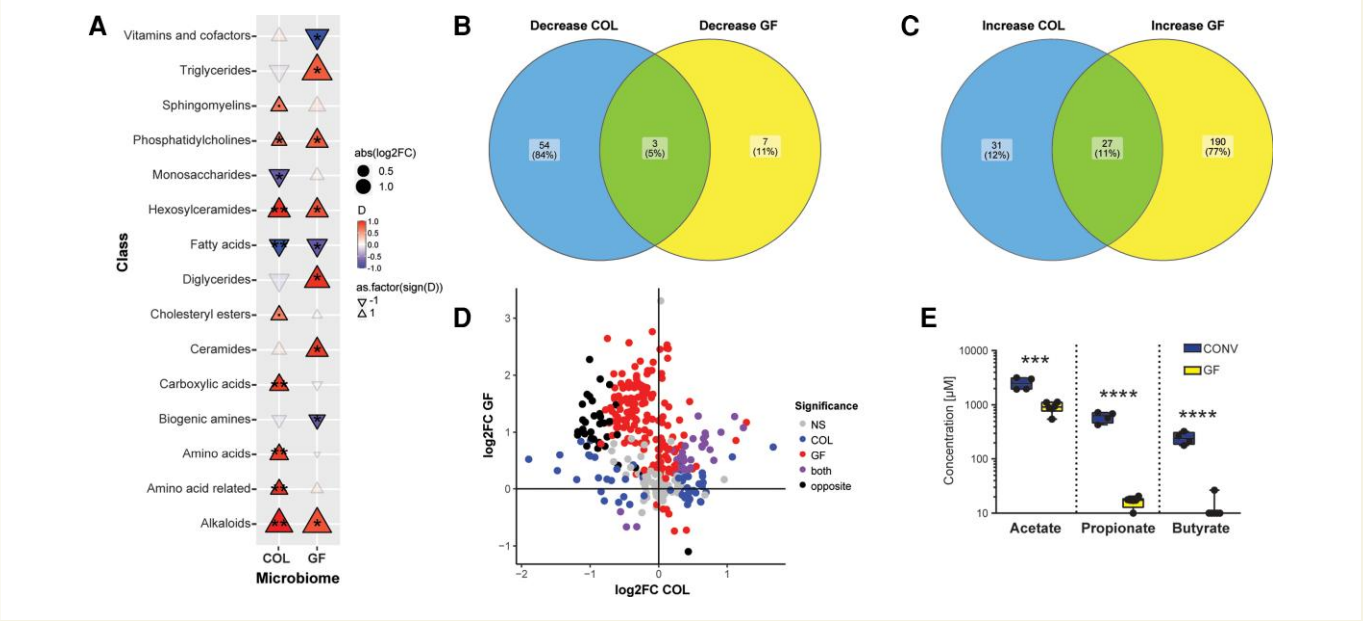

Figure 5 Microbiome heavily influences the metabolome in response to HTN. (*A*) Using the Biocrates MxP500 Quant kit, serum metabolites were analysed from GF and COL mice. Metabolites were grouped by class to demonstrate the overall effect on the serum metabolome (Sham GF $n = 5$, Sham COL $n = 5$, GF + HTN $n = 10$, COL + HTN $n = 11$). Effect size [Cliff's delta (*D*)] is shown to demonstrate the effect of HTN relative to the respective sham group in GF and COL. Colour and triangle direction indicates effect size. Size indicates log2-transformed fold change (Log2FC) of HTN mice compared with the respective sham group. Significance was calculated using the Mann–Whitney *U*-test and was FDR-corrected using the Benjamini–Hochberg procedure to account for multiple testing. Markers for significant Q-values are superimposed, and transparency indicates non-significant effects. °$q < 0.1$, *$q < 0.05$, **$q < 0.01$. For (*B*) and (*C*), individual metabolites rather than metabolite classes within the GF and COL group were compared using the effect size calculation listed in (*A*, see Supplementary material online, *Table S11*). Those metabolites which were significantly altered in the sham to HTN comparison, as tested using the Mann–Whitney *U*-test with Benjamini–Hochberg FDR correction were selected and separated based on the directionality of their shift. Metabolites which decreased (*B*) or increased (*C*) in HTN relative to sham are compared between the COL and GF conditions using a Venn diagram. The number of metabolites and the percentage within each subcategory are overlayed. In (*D*) significant changes to individual metabolites (points) are shown in GF (*y*-axis) and COL (*x*-axis) as log2-fold changes in response to HTN. Metabolites exclusively significantly regulated in GF or in COL are shown in red and blue, respectively. Purple points indicate metabolites significantly regulated similarly in GF and COL (significant in both and same trajectory), while black points indicate metabolites regulated significant in both groups but with opposite trajectories. Grey points are metabolites which were reliably measured but not significantly altered in either group. (*E*) Faecal SCFA from GF or CONV mice demonstrates the absence of potent anti-hypertensive metabolites butyrate and propionate in the GF setting (GF $n = 6$, CONV $n = 4$). Significance was tested using unpaired two-tailed Student's *t*-test (***$P \leq 0.001$, ****$P \leq 0.0001$). LC-MS, liquid chromatography-mass spectrometry; FIA-MS, flow injection analysis-mass spectrometry.

cytokines. Therefore, we performed an *in vitro* Th17 polarization of naive T-cells from GF and CONV mice (which were used in place of COL due to ease of accessibility) in the presence or absence of Ang II. Naive T-cells from GF mice more readily polarized towards Th17 cells than cells from CONV mice, particularly in the presence of Ang II (*Figure 6G*). To demonstrate that the conditions for the polarization of Th17 cells indeed exist *in vivo*, we quantified the expression of each of the Th17-polarizing cytokines (Il-6, Il-1b, and TGFb) by qPCR from kidney (see Supplementary material online, *Figure S9A*, and *Figure 3A*) and heart (see Supplementary material online, *Figure S9B*, and *Figure 3C*) tissue. These key cytokines were increased upon HTN. The comparison of effect sizes (*Figure 3A and C*) often indicated larger effects of HTN in GF mice. We suspected that the reason naive CD4+ T-cells isolated from CONV mice were less inducible toward Th17 in the presence of Ang II may be due to the priming of immune cells by SCFA in the *in vivo* microenvironment. To test this hypothesis, prior to Th17 induction in the presence of Ang II, naive CD4+ cells were pre-treated for 24 h with the SCFA butyrate and propionate. While the pre-treatment did not affect the induction of Th17 in CONV, SCFA pre-treatment prevented the enhanced Th17 induction of naive T-cells from GF mice (*Figure 6H*).

In summary, our *in vitro* findings suggest that the different preconditioning of naive T-cells within GF and COL mice may impact polarization into pro-inflammatory effector T-cells and thus severity of target organ damage. We anticipate that this effect contributes to our *in vivo* findings, where the absence of microbes and microbiota-derived metabolites like SCFA had a potent impact on immune cells relevant in HTN and cardiorenal damage.

4. Discussion

Gut microbial dysbiosis associates with HTN in humans[5,32] and in rodent models.[5,32–34] Faecal microbiota transplantation from hypertensive patients into mice has also been shown to induce an increase in BP.[32] However, few studies have focused on the overall contribution of the microbiome to the pathogenesis of HTN, such that it may be contextualized relative to other known contributors to hypertensive disease

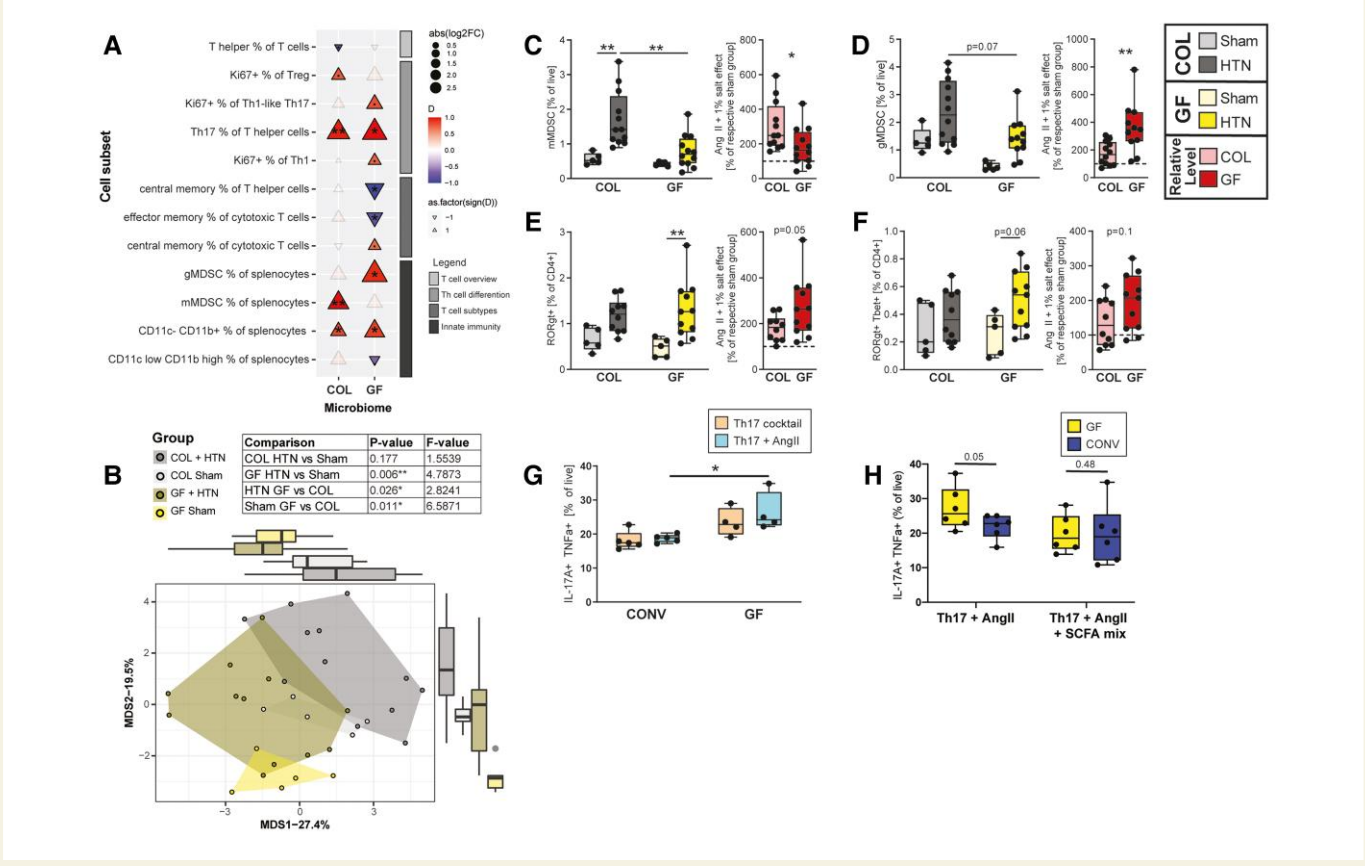

Figure 6 Colonization status influences the inflammatory reaction to HTN. Unless otherwise stated, GF Sham $n = 5$, GF + HTN $n = 12$, COL Sham $n = 5$, COL + HTN $n = 12$. (*A*) Several unique immune cell subsets were measured from the spleen, as a proxy measure of systemic inflammation. Effect size (Cliff's delta [D]) is shown to demonstrate the effect of HTN relative to the respective sham group in GF and COL. Colour and triangle direction indicates effect size. Size indicates log2-transformed fold change (Log2FC) of HTN induction compared with the respective sham group. Significance was calculated using the Mann–Whitney *U*-test and was FDR-corrected using the Benjamini–Hochberg procedure to account for multiple testing. Markers for significant Q-values are superimposed, and transparency indicates non-significant effects. °$q < 0.1$, *$q < 0.05$, **$q < 0.01$. Immune cell subsets are organized by sub-category (Innate immunity and T-cell overview, differentiation, and subtypes) and subsets, and cell types where no significant effect in either GF or COL was found are not shown. (*B*) PCoA was performed based on Euclidean distance scaling of immune cell abundances to demonstrate the dissimilarities between study groups. Pairwise comparisons between groups were performed using PERMANOVA and reported in the inset table. Monocytic MDSCs (mMDSC, *C*) and granulocytic MDSCs (gMDSC, *D*), as well as Th17 (*E*) and Th1-like Th17 cells (*F*) from the spleen are shown as boxplots on the left. (*G*) naive CD4+ T-cells from mesenteric lymph nodes of either GF of CONV mice, polarized *in vitro* towards a Th17 using a cocktail of IL-1β, TGFβ, and IL-6 with or without Ang II (GF $n = 4$, CONV $n = 5$). In (H) naive CD4+ T-cells were pre-treated with 1 mM SCFA mix (0.5 mM of each butyrate and propionate) or 1 mM NaCl. Subsequently, the pre-treatment was removed, and cells were polarized toward Th17 in the presence of Ang II as described in G (GF $n = 6$, CONV $n = 6$). To the left in (*C*–*G*), two-way ANOVA and *post hoc* Sidak multiple comparison's test was used to test significance. To the right in (*C*–*F*), the relative change induced by Ang II + 1% NaCl in comparison with the respective sham group was tested using an unpaired two-tailed *t*-test. No change (100%) depicted as dotted line. In (*H*) for the Th17 + Ang II and Th17 + Ang II + SCFA mix a one-tailed *t*-test was performed per group, as a pre-specified hypothesis from *Figure 6G* was tested. For all plots in (*C*–*G*), *P*-values are as follows; *$P \leq 0.05$, **$P \leq 0.01$.

burden. Here we show in a presence/absence scenario, that the microbiota has a potent effect on HTN-induced cardiac and renal damage in mice. GF mice showed a stronger adverse response to HTN than their COL littermates. Interestingly, the kidney seems to be more sensitive to changes in microbial status than the heart. Finally, we propose that the altered inflammatory response in GF mice contributes to their aggravated phenotype in HTN.

We have shown robustly that the kidney damage within GF mice upon HTN is comparatively more severe than the damage experienced by their COL littermates. Some of the larger effects in our univariate analysis may be related to the slightly lower baseline level of putative markers for kidney damage within sham GF mice compared with sham COL, though these groups do not significantly differ. We surmise that the baseline differences between GF and COL mice are likely due to the immunological uniqueness of GF mice, which has been documented in the literature.[27] Indeed, across renal damage, fibrosis and inflammation markers, we consistently saw a significant effect of HTN selectively in the GF group (*Figure 3A*). Furthermore, we show on a multivariate level that the difference between sham GF and GF + HTN mice for the composite of kidney parameters is significant, while the equivalent comparison within the COL mice is insignificant (*Figure 3C*). Consistent with other inflammatory markers, we show an increase of infiltrating macrophages (F4/80+ cells, *Figure 1E*) in GF + HTN kidneys, as well as the increased expression of *Ccl2* (see Supplementary material online,

Figure S3A), which has been implicated as a major player in worsening kidney damage in mice[35] and humans.[36] Infiltrating macrophages during renal injury are known to contribute to the secretion of cytokines like IL-1β, which enhances the activation and differentiation of Th17 cells.[37] A previous study additionally showed that SCFA-treatment in ischaemia-reperfusion injury (IRI) radically reduced kidney *Ccl2*, *Il-1b*, and associated kidney damage.[38] SCFA have been shown to have anti-inflammatory properties in several cell types,[39–42] which could contribute to the lessened damage in COL mice, since only mice harbouring microbiota have significant SCFA production within the GI tract (*Figure 5C*). Our results are highly compatible with previous studies showing that GF status exacerbates kidney damage in the context of IRI[43] and adenine-induced chronic kidney disease.[21,44]

Intriguingly, we found that the cardiac phenotype was less influenced by the microbial status of the host. Here we have shown that particularly for markers of fibrosis (*Figure 3B*), regardless of the microbiome status, the mice developed significant injury. For CD8+ T-cells, F4/80+ macrophages and overall CD45+ leukocytes, we observed significant changes in GF and COL mice, although GF mice tended to show a higher fold change in response to HTN (see Supplementary material online, *Table S2*). Despite these similarities, both cardiac hypertrophy (*Figure 2A*) and left ventricular mass-to-tibia length (*Figure 2B*) were significantly altered upon HTN induction in the GF but not COL mice. Nonetheless, our data suggest that the kidney, more so than the heart, represents a subspace of hypertensive target organ damage, which is more susceptible to microbial colonization. It is conceivable that cardiac damage could be further exacerbated as renal function declines. Thus, the gut microbiota could be added as an important modulator of the well-known cardiorenal axis. Further research to follow up this idea is required, perhaps using several iterations of variations to a defined community of microbes, to test the universality of this hypothesis.

Metabolites of microbial origin, some of which are known to be associated with CVD and accumulate in chronic kidney disease,[16,17] were measurable within the serum metabolome of our COL but not our GF mice, such as IS and TMAO (see Supplementary material online, *Figure S1D*). Our results very clearly indicate that GF mice experience robust kidney damage to a greater extent than COL mice, despite GF mice being devoid of these harmful metabolites. However, we suggest that the reason COL mice experience less overall damage is likely due to the presence of SCFA. We and others have shown the potent effect of SCFA in mouse models.[13,14] Here we have shown again, for a representative set of animals, that SCFA are depleted in GF mice (*Figure 5C*). We hypothesize that the potency of SCFA in COL mice counterbalances the presence of IS and TMAO. Further research on this topic is required to definitively conclude the effects of the co-occurrence of these various metabolites of microbial origin.

Furthermore, we show that systemic inflammatory response to HTN is altered by colonization status. MSDC, which represent an important subset of innate anti-inflammatory cells in HTN,[9] reacted differently GF mice compared with COL (*Figure 6C and D*). Additionally, we found that Th17 cells were increased during HTN in GF mice (*Figure 6E*). Th1-like Th17 cells, which are known to be pathogenic, trended towards enrichment in GF + HTN mice (*Figure 6F*). We wanted to explore *in vitro* that naive T-cells from GF mice were more sensitive to polarizing cytokines and Ang II. We found that upon polarization, naive T-cells from GF mice skewed more towards Th17, particularly when Ang II was added (*Figure 6G*). As it has been recently demonstrated that the SCFA propionate can decrease the rate of Th17 cell differentiation,[41,42] we suspected that this could be part of the reason naive cells from COL mice were less inducible toward Th17. Indeed, when we pre-treated naive CD4+ T-cells with butyrate and propionate, we observed a decline in Th17 inducibility in the presence of Ang II in GF; an effect that was not seen in cells isolated from CONV mice (*Figure 6H*). Recently, Krebs and colleagues showed that the development of Th17 cells in the kidney is dependent on the cytokine micromilieu and can be blocked with specific antibodies against IL-1b and IL-6.[45] We also could show that the polarization conditions used in our Th17 *in vitro* assay were practically available *in vivo*, and the expression of each polarizing cytokine was increased within heart and kidney tissue of hypertensive mice.

To our knowledge, one study similar to ours exists within the literature, published by Karbach *et al.*[46] It is clear from the extensive phenotyping performed in our study that our findings were not congruent with their data, where they showed that GF mice were protected from developing HTN and related vascular damage. Though this was initially a surprise, upon further examination, there are two likely scenarios that may explain this. First, the protocol of our experiments did differ from one another. The study from Karbach and colleagues compared GF mice with conventionally raised mice, whereas we compared GF mice with littermates that had been colonized early in life. Therefore, our study was able to account for known genetic drifts in gnotobiotic colonies. Additionally, Ang II infusion was only performed for seven days, while we studied a more chronic phenotype. Furthermore, our mice ate different diets, and as Kaye and colleagues recently demonstrated, the composition of the diet can have a profound impact on the resultant hypertensive phenotype.[47] Second, it is highly likely that the microbiome used in our study and in the study by Karbach and colleagues may be distinct from one another. Incongruencies like ours have also been found in other contexts. The comparison of microbiome-rich and GF mice in one study showed the amelioration of an IRI of the kidney by the microbiome,[43] where another study demonstrated the opposite effect.[48]

To investigate the second scenario further, we hypothesized that the microbiome background used in any given study might have drastic implications for the study outcome. Our group and others have shown that microbially-produced metabolites have a potent effect on the pathogenesis of HTN.[5,13,14,49] In reference to that, if the microbiota itself were to change, we expect the circulating metabolites to be likewise altered within the host. Unfortunately, the study from Karbach *et al.*[46] did not include any information regarding the microbiome and metabolome of their microbiota-rich mice. Although, we did find a recent study from Cheema and Pluznick[20] where these data were made available, but their phenotypic data is not reported.[20] Nevertheless, to test our hypothesis regarding the putative comparability of the colonizing microbiome between studies, and the impact this may have on resultant study outcome, we decided to compare our microbiome and metabolome with the published data from Cheema and Pluznick. To compare the microbiomes from these two studies, we re-annotated our shotgun microbiome sequencing data such that it would be comparable to the 16s rDNA sequencing data from Cheema and Pluznick. The microbiome of CONV between the two studies were starkly contrasting in sham and HTN mice (shown as a multivariate PCoA plot derived from genus level information from each of the studies, see Supplementary material online, *Figure S10A*). We surmised that because of the lack of overlapping microbiome signatures within our study and the Pluznick dataset, that the metabolome signal would likewise be dichotomous. We compared the serum metabolome dataset from the two studies by using metabolites which could be measured in both studies from all COL and GF mice. We found that interestingly, there was significantly less distance

between the effect of HTN on individual metabolites within the serum metabolome of GF mice from these two studies than in the equivalent COL mice comparison (see Supplementary material online, *Figure S10B and C*). This result suggests that the congruence of the serum metabolome in GF groups within these two datasets is higher than the COL groups. These exploratory data support the idea that the structure of the implanted microbiome has a measurable impact on serum metabolome alterations in response to HTN. Because of our and others' findings regarding the importance of microbial metabolites in HTN, we believe that this could be a driving factor behind the contradictory phenotypic results of our study compared with the data from Karbach *et al.*[46] It is nonetheless critical in future studies for the microbiome to be well documented and openly accessible to avoid questions regarding the reproducibility of existing studies.

5. Conclusion

We have shown that the microbiota has a profound effect on hypertensive disease pathogenesis. Furthermore, we have shown that GF mice, when compared with their colonized littermates, experienced an aggravation of target organ damage, which was more distinct in the kidney than in the heart. Additionally, we demonstrated that the metabolome is influenced significantly by the microbiome used for experimentation, which underscores the need for standardization of experimentation and reporting within the field. The immunophenotype of HTN mice, and in particular, the alteration of MDSC and Th17 cells, which have been previously implicated in HTN, give us some indication of how GF mice may have developed an exacerbated hypertensive phenotype in our study. *In vitro*, SCFA rescued the pro-inflammatory phenotype of T-cells isolated from GF mice. We propose that the COL mice were protected from damage in comparison with their GF counterparts due to the absence of the potent anti-inflammatory SCFA metabolites under GF conditions.

Supplementary material

Supplementary material is available at *Cardiovascular Research* online.

Authors' Contributions

N.W., D.N.M., and H.B. designed the study. E.G.A., H.B., A.R., G.N., D.T., A.Y., C.Z., L. Y., L.M., A.M., A.P., and N.W. performed animal experiments and analysed the data. A.F.R, M.T., and M.B. performed *in vivo* BP measurement. C.-Y.C., U.L., and T.U.P.B. performed the microbiome analysis. E.G.A., R.F.G., S.K., and J.A.K. performed and analysed the metabolomics experiments. S.K.F. helped with data analysis and interpretation. E.G.A., N.W., H.B., and D.N.M. wrote the manuscript with input from all authors.

Acknowledgments

We thank Petra Voss, Ilona Kramer, May-Britt Köhler, Jana Czychi, Ute Gerhardt, Alina Eisenberger, Martin Taube, and Stefanie Schelenz for their technical assistance.

Conflict of interest: none declared.

Funding

N.W. is supported by the European Research Council (ERC) under the European Union's Horizon 2020 research and innovation programme (852796) and by a grant from the Corona-Stiftung, Deutsches Stiftungszentrum, Essen, Germany. A.P., N.W., D.N.M., and S.K.F. are supported by the Deutsche Forschungsgemeinschaft (DFG, German Research Foundation) Projektnummer 394046635—SFB 1365. The DZHK (German Centre for Cardiovascular Research, 81Z1100101) supported D.N.M. N.W. was participant in the Clinician Scientist Programme funded by the Berlin Institute of Health (BIH).

Data availability

The data underlying this article are available in the article and in its online supplementary material. The microbiome data underlying this article are available in NCBI database and can be accessed as BioProject PRJNA812410. The metabolomics data underlying this article are available via FigShare, please see Supplementary material online, *Table S10* for access links.

References

1. Ezzati M, Riboli E. Behavioral and dietary risk factors for noncommunicable diseases. *N Engl J Med* 2013;**369**:954–964.
2. Avery EG, Bartolomaeus H, Maifeld A, Marko L, Wiig H, Wilck N, Rosshart SP, Forslund SK, Muller DN. The gut microbiome in hypertension: recent advances and future perspectives. *Circ Res* 2021;**128**:934–950.
3. Madhur MS, Elijovich F, Alexander MR, Pitzer A, Ishimwe J, Van Beusecum JP, Patrick DM, Smart CD, Kleyman TR, Kingery J, Peck RN, Laffer CL, Kirabo A. Hypertension: do inflammation and immunity hold the key to solving this epidemic? *Circ Res* 2021;**128**:908–933.
4. Verhaar BJH, Collard D, Prodan A, Levels JHM, Zwinderman AH, Backhed F, Vogt L, Peters MJL, Muller M, Nieuwdorp M, van den Born BH. Associations between gut microbiota, faecal short-chain fatty acids, and blood pressure across ethnic groups: the HELIUS study. *Eur Heart J* 2020;**41**:4259–4267.
5. Wilck N, Matus MG, Kearney SM, Olesen SW, Forslund K, Bartolomaeus H, Haase S, Mahler A, Balogh A, Marko L, Vvedenskaya O, Kleiner FH, Tsvetkov D, Klug L, Costea PI, Sunagawa S, Maier L, Rakova N, Schatz V, Neubert P, Fratzer C, Krannich A, Gollasch M, Grohme DA, Corte-Real BF, Gerlach RG, Basic M, Typas A, Wu C, Titze JM, Jantsch J, Boschmann M, Dechend R, Kleinewietfeld M, Kempa S, Bork P, Linker RA, Alm EJ, Muller DN. Salt-responsive gut commensal modulates TH17 axis and disease. *Nature* 2017;**551**:585–589.
6. Yang T, Santisteban MM, Rodriguez V, Li E, Ahmari N, Carvajal JM, Zadeh M, Gong M, Qi Y, Zubcevic J, Sahay B, Pepine CJ, Raizada MK, Mohamadzadeh M. Gut dysbiosis is linked to hypertension. *Hypertension* 2015;**65**:1331–1340.
7. Madhur MS, Lob HE, McCann LA, Iwakura Y, Blinder Y, Guzik TJ, Harrison DG. Interleukin 17 promotes angiotensin II-induced hypertension and vascular dysfunction. *Hypertension* 2010;**55**:500–507.
8. Marko L, Kvakan H, Park JK, Qadri F, Spallek B, Binger KJ, Bowman EP, Kleinewietfeld M, Fokuhl V, Dechend R, Muller DN. Interferon- γ signaling inhibition ameliorates angiotensin II-induced cardiac damage. *Hypertension* 2012;**60**:1430–1436.
9. Shah KH, Shi P, Giani JF, Janjulia T, Bernstein EA, Li Y, Zhao T, Harrison DG, Bernstein KE, Shen XZ. Myeloid suppressor cells accumulate and regulate blood pressure in hypertension. *Circ Res* 2015;**117**:858–869.
10. Ivanov II, Atarashi K, Manel N, Brodie EL, Shima T, Karaoz U, Wei D, Goldfarb KC, Santee CA, Lynch SV, Tanoue T, Imaoka A, Itoh K, Takeda K, Umesaki Y, Honda K, Littman DR. Induction of intestinal Th17 cells by segmented filamentous bacteria. *Cell* 2009;**139**:485–498.
11. Zaccone P, Raine T, Sidobre S, Kronenberg M, Mastroeni P, Cooke A. Salmonella typhimurium infection halts development of type 1 diabetes in NOD mice. *Eur J Immunol* 2004;**34**:3246–3256.
12. Tan J, McKenzie C, Potamitis M, Thorburn AN, Mackay CR, Macia L. The role of short-chain fatty acids in health and disease. *Adv Immunol* 2014;**121**:91–119.
13. Marques FZ, Nelson E, Chu PY, Horlock D, Fiedler A, Ziemann M, Tan JK, Kuruppu S, Rajapakse NW, El-Osta A, Mackay CR, Kaye DM. High-fiber diet and acetate supplementation change the gut microbiota and prevent the development of hypertension and heart failure in hypertensive mice. *Circulation* 2017;**135**:964–977.
14. Bartolomaeus H, Balogh A, Yakoub M, Homann S, Marko L, Hoges S, Tsvetkov D, Krannich A, Wundersitz S, Avery EG, Haase N, Kraker K, Hering L, Maase M, Kusche-Vihrog K, Grandoch M, Fielitz J, Kempa S, Gollasch M, Zhumadilov Z, Kozhakhmetov S, Kushugulova A, Eckardt KU, Dechend R, Rump LC, Forslund SK, Muller DN, Stegbauer J, Wilck N. Short-chain fatty acid propionate protects from hypertensive cardiovascular damage. *Circulation* 2019;**139**:1407–1421.
15. Poll BG, Cheema MU, Pluznick JL. Gut microbial metabolites and blood pressure regulation: focus on SCFAs and TMAO. *Physiology (Bethesda)* 2020; **35**:275–284.
16. Zhu W, Gregory JC, Org E, Buffa JA, Gupta N, Wang Z, Li L, Fu X, Wu Y, Mehrabian M, Sartor RB, McIntyre TM, Silverstein RL, Tang WHW, DiDonato JA, Brown JM, Lusis AJ,

Hazen SL. Gut microbial metabolite TMAO enhances platelet hyperreactivity and thrombosis risk. *Cell* 2016;**165**:111–124.
17. Nakano T, Katsuki S, Chen M, Decano JL, Halu A, Lee LH, Pestana DVS, Kum AST, Kuromoto RK, Golden WS, Boff MS, Guimaraes GC, Higashi H, Kauffman KJ, Maejima T, Suzuki T, Iwata H, Barabasi AL, Aster JC, Anderson DG, Sharma A, Singh SA, Aikawa E, Aikawa M. Uremic toxin indoxyl sulfate promotes proinflammatory macrophage activation via the interplay of OATP2B1 and Dll4-notch signaling. *Circulation* 2019;**139**:78–96.
18. Marko L, Park JK, Henke N, Rong S, Balogh A, Klamer S, Bartolomaeus H, Wilck N, Ruland J, Forslund SK, Luft FC, Dechend R, Muller DN. B-cell lymphoma/leukaemia 10 and angiotensin II-induced kidney injury. *Cardiovasc Res* 2020;**116**:1059–1070.
19. Leelahavanichkul A, Yan Q, Hu X, Eisner C, Huang Y, Chen R, Mizel D, Zhou H, Wright EC, Kopp JB, Schnermann J, Yuen PS, Star RA. Angiotensin II overcomes strain-dependent resistance of rapid CKD progression in a new remnant kidney mouse model. *Kidney Int* 2010;**78**:1136–1153.
20. Cheema MU, Pluznick JL. Gut microbiota plays a central role to modulate the plasma and fecal metabolomes in response to angiotensin II. *Hypertension* 2019;**74**:184–193.
21. Mishima E, Ichijo M, Kawabe T, Kikuchi K, Akiyama Y, Toyohara T, Suzuki T, Suzuki C, Asao A, Ishii N, Fukuda S, Abe T. Germ-free conditions modulate host purine metabolism, exacerbating adenine-induced kidney damage. *Toxins (Basel)* 2020;**12**:547.
22. Richards DA, Aronovitz MJ, Calamaras TD, Tam K, Martin GL, Liu P, Bowditch HK, Zhang P, Huggins GS, Blanton RM. Distinct phenotypes induced by three degrees of transverse aortic constriction in mice. *Sci Rep* 2019;**9**:5844.
23. Joe B, McCarthy CG, Edwards JM, Cheng X, Chakraborty S, Yang T, Golonka RM, Mell B, Yeo JY, Bearss NR, Furtado J, Saha P, Yeoh BS, Vijay-Kumar M, Wenceslau CF. Microbiota introduced to germ-free rats restores vascular contractility and blood pressure. *Hypertension* 2020;**76**:1847–1855.
24. Edwards JM, Roy S, Tomcho JC, Schreckenberger ZJ, Chakraborty S, Bearss NR, Saha P, McCarthy CG, Vijay-Kumar M, Joe B, Wenceslau CF. Microbiota are critical for vascular physiology: germ-free status weakens contractility and induces sex-specific vascular remodeling in mice. *Vascul Pharmacol* 2020;**125-126**:106633.
25. Mattson DL. Comparison of arterial blood pressure in different strains of mice. *Am J Hypertens* 2001;**14**:405–408.
26. Hoverstad T, Midtvedt T. Short-chain fatty acids in germfree mice and rats. *J Nutr* 1986;**116**:1772–1776.
27. Smith K, McCoy KD, Macpherson AJ. Use of axenic animals in studying the adaptation of mammals to their commensal intestinal microbiota. *Semin Immunol* 2007;**19**:59–69.
28. Kamali AN, Noorbakhsh SM, Hamedifar H, Jadidi-Niaragh F, Yazdani R, Bautista JM, Azizi G. A role for Th1-like Th17 cells in the pathogenesis of inflammatory and autoimmune disorders. *Mol Immunol* 2019;**105**:107–115.
29. Coit P, Dozmorov MG, Merrill JT, McCune WJ, Maksimowicz-McKinnon K, Wren JD, Sawalha AH. Epigenetic reprogramming in naive CD4+ T cells favoring T Cell activation and non-Th1 effector T cell immune response as an early event in lupus flares. *Arthritis Rheumatol* 2016;**68**:2200–2209.
30. Altorok N, Coit P, Hughes T, Koelsch KA, Stone DU, Rasmussen A, Radfar L, Scofield RH, Sivils KL, Farris AD, Sawalha AH. Genome-wide DNA methylation patterns in naive CD4+ T cells from patients with primary Sjogren's syndrome. *Arthritis Rheumatol* 2014;**66**:731–739.
31. Heninger AK, Eugster A, Kuehn D, Buettner F, Kuhn M, Lindner A, Dietz S, Jergens S, Wilhelm C, Beyerlein A, Ziegler AG, Bonifacio E. A divergent population of autoantigen-responsive CD4(+) T cells in infants prior to beta cell autoimmunity. *Sci Transl Med* 2017;**9**:eaaf8848.
32. Li J, Zhao F, Wang Y, Chen J, Tao J, Tian G, Wu S, Liu W, Cui Q, Geng B, Zhang W, Weldon R, Auguste K, Yang L, Liu X, Chen L, Yang X, Zhu B, Cai J. Gut microbiota dysbiosis contributes to the development of hypertension. *Microbiome* 2017;**5**:14.
33. Adnan S, Nelson JW, Ajami NJ, Venna VR, Petrosino JF, Bryan RM Jr, Durgan DJ. Alterations in the gut microbiota can elicit hypertension in rats. *Physiol Genomics* 2017;**49**:96–104.
34. Santisteban MM, Qi Y, Zubcevic J, Kim S, Yang T, Shenoy V, Cole-Jeffrey CT, Lobaton GO, Stewart DC, Rubiano A, Simmons CS, Garcia-Pereira F, Johnson RD, Pepine CJ, Raizada MK. Hypertension-linked pathophysiological alterations in the gut. *Circ Res* 2017;**120**:312–323.
35. Kashyap S, Osman M, Ferguson CM, Nath MC, Roy B, Lien KR, Nath KA, Garovic VD, Lerman LO, Grande JP. Ccl2 deficiency protects against chronic renal injury in murine renovascular hypertension. *Sci Rep* 2018;**8**:8598.
36. Eardley KS, Zehnder D, Quinkler M, Lepenies J, Bates RL, Savage CO, Howie AJ, Adu D, Cockwell P. The relationship between albuminuria, MCP-1/CCL2, and interstitial macrophages in chronic kidney disease. *Kidney Int* 2006;**69**:1189–1197.
37. Pindjakova J, Hanley SA, Duffy MM, Sutton CE, Weidhofer GA, Miller MN, Nath KA, Mills KH, Ceredig R, Griffin MD. Interleukin-1 accounts for intrarenal Th17 cell activation during ureteral obstruction. *Kidney Int* 2012;**81**:379–390.
38. Andrade-Oliveira V, Amano MT, Correa-Costa M, Castoldi A, Felizardo RJ, de Almeida DC, Bassi EJ, Moraes-Vieira PM, Hiyane MI, Rodas AC, Peron JP, Aguiar CF, Reis MA, Ribeiro WR, Valduga CJ, Curi R, Vinolo MA, Ferreira CM, Camara NO. Gut bacteria products prevent AKI induced by ischemia-reperfusion. *J Am Soc Nephrol* 2015;**26**:1877–1888.
39. Singh N, Thangaraju M, Prasad PD, Martin PM, Lambert NA, Boettger T, Offermanns S, Ganapathy V. Blockade of dendritic cell development by bacterial fermentation products butyrate and propionate through a transporter (Slc5a8)-dependent inhibition of histone deacetylases. *J Biol Chem* 2010;**285**:27601–27608.
40. Wang F, Liu J, Weng T, Shen K, Chen Z, Yu Y, Huang Q, Wang G, Liu Z, Jin S. The inflammation induced by lipopolysaccharide can be mitigated by short-chain fatty acid. Butyrate, through upregulation of IL;10, in septic shock. *Scand J Immunol* 2017;**85**:258–263.
41. Duscha A, Gisevius B, Hirschberg S, Yissachar N, Stangl GI, Eilers E, Bader V, Haase S, Kaisler J, David C, Schneider R, Troisi R, Zent D, Hegelmaier T, Dokalis N, Gerstein S, Del Mare-Roumani S, Amidror S, Staszewski O, Poschmann G, Stuhler K, Hirche F, Balogh A, Kempa S, Trager P, Zaiss MM, Holm JB, Massa MG, Nielsen HB, Faissner A, Lukas C, Gatermann SG, Scholz M, Przuntek H, Prinz M, Forslund SK, Winklhofer KF, Muller DN, Linker RA, Gold R, Haghikia A. Propionic acid shapes the multiple sclerosis disease course by an immunomodulatory mechanism. *Cell* 2020;**180**:1067–1080.e16.
42. Haghikia A, Jorg S, Duscha A, Berg J, Manzel A, Waschbisch A, Hammer A, Lee DH, May C, Wilck N, Balogh A, Ostermann AI, Schebb NH, Akkad DA, Grohme DA, Kleinewietfeld M, Kempa S, Thone J, Demir S, Muller DN, Gold R, Linker RA. Dietary fatty acids directly impact central nervous system autoimmunity via the small intestine. *Immunity* 2015;**43**:817–829.
43. Jang HR, Gandolfo MT, Ko GJ, Satpute S, Racusen L, Rabb H. Early exposure to germs modifies kidney damage and inflammation after experimental ischemia-reperfusion injury. *Am J Physiol Renal Physiol* 2009;**297**:F1457–F1465.
44. Mishima E, Fukuda S, Mukawa C, Yuri A, Kanemitsu Y, Matsumoto Y, Akiyama Y, Fukuda NN, Tsukamoto H, Asaji K, Shima H, Kikuchi K, Suzuki C, Suzuki T, Tomioka Y, Soga T, Ito S, Abe T. Evaluation of the impact of gut microbiota on uremic solute accumulation by a CE-TOFMS-based metabolomics approach. *Kidney Int* 2017;**92**:634–645.
45. Krebs CF, Reimers D, Zhao Y, Paust HJ, Bartsch P, Nunez S, Rosemblatt MV, Hellmig M, Kilian C, Borchers A, Enk LUB, Zinke M, Becker M, Schmid J, Klinge S, Wong MN, Puelles VG, Schmidt C, Bertram T, Stumpf N, Hoxha E, Meyer-Schwesinger C, Lindenmeyer MT, Cohen CD, Rink M, Kurts C, Franzenburg S, Koch-Nolte F, Turner JE, Riedel JH, Huber S, Gagliani N, Huber TB, Wiech T, Rohde H, Bono MR, Bonn S, Panzer U, Mittrucker HW. Pathogen-induced tissue-resident memory TH17 (TRM17) cells amplify autoimmune kidney disease. *Sci Immunol* 2020;**5**:eaba4163.
46. Karbach SH, Schonfelder T, Brandao I, Wilms E, Hormann N, Jackel S, Schuler R, Finger S, Knorr M, Lagrange J, Brandt M, Waisman A, Kossmann S, Schafer K, Munzel T, Reinhardt C, Wenzel P. Gut microbiota promote angiotensin II-induced arterial hypertension and vascular dysfunction. *J Am Heart Assoc* 2016;**5**:e003698.
47. Kaye DM, Shihata WA, Jama HA, Tsyganov K, Ziemann M, Kiriazis H, Horlock D, Vijay A, Giam B, Vinh A, Johnson C, Fiedler A, Donner D, Snelson M, Coughlan MT, Phillips S, Du XJ, El-Osta A, Drummond G, Lambert GW, Spector TD, Valdes AM, Mackay CR, Marques FZ. Deficiency of prebiotic fiber and insufficient signaling through gut metabolite-sensing receptors leads to cardiovascular disease. *Circulation* 2020;**141**:1393–1403.
48. Emal D, Rampanelli E, Stroo I, Butter LM, Teske GJ, Claessen N, Stokman G, Florquin S, Leemans JC, Dessing MC. Depletion of gut microbiota protects against renal ischemia-reperfusion injury. *J Am Soc Nephrol* 2017;**28**:1450–1461.
49. Heianza Y, Ma W, Manson JE, Rexrode KM, Qi L. Gut microbiota metabolites and risk of major adverse cardiovascular disease events and death: a systematic review and meta-analysis of prospective studies. *J Am Heart Assoc* 2017;**6**:e004947.

Translational perspective

To assess the potential of microbiota-targeted interventions to prevent organ damage in hypertension, an accurate quantification of microbial influence is necessary. We provide evidence that the development of hypertensive organ damage is dependent on colonization status and suggest that a healthy microbiota provides anti-hypertensive immune and metabolic signals to the host. In the absence of normal symbiotic host-microbiome interactions, hypertensive damage to the kidney in particular is exacerbated. We suggest that hypertensive patients experiencing perturbations to the microbiota, which are common in CVD, may be at a greater risk for target-organ damage than those with a healthy microbiome.